Organic & Biomolecular Chemistry

Cite this: *Org. Biomol. Chem.*, 2012, **10**, 1571

www.rsc.org/obc

PAPER

Analogues of uracil nucleosides with intrinsic fluorescence (NIF-analogues): synthesis and photophysical properties†

Meirav Segal and Bilha Fischer*

Received 7th September 2011, Accepted 17th November 2011
DOI: 10.1039/c1ob06536j

Uridine cannot be utilized as fluorescent probe due to its extremely low quantum yield. For improving the uracil fluorescence characteristics we extended the natural chromophore at the C5 position by coupling substituted aromatic rings directly or *via* an alkenyl or alkynyl linker to create fluorophores. Extension of the uracil base was achieved by treating 5-I-uridine with the appropriate boronic acid under the Suzuki coupling conditions. Analogues containing an alkynyl linker were obtained from 5-I-uridine and the suitable boronic acid in a Sonogashira coupling reaction. The uracil fluorescent analogues proposed here were designed to satisfy the following requirements: a minimal chemical modification at a position not involved in base-pairing, resulting in relatively long absorption and emission wavelengths and high quantum yield. 5-((4-Methoxy-phenyl)-*trans*-vinyl)-2′-deoxy-uridine, **6b**, was found to be a promising fluorescent probe. Probe **6b** exhibits a quantum yield that is 3000-fold larger than that of the natural chromophore (Φ 0.12), maximum emission (478 nm) which is 170 nm red shifted as compared to uridine, and a Stokes shift of 143 nm. In addition, since probe **6b** adopts the *anti* conformation and *S* sugar puckering favored by B-DNA, it makes a promising nucleoside analogue to be incorporated in an oligonucleotide probe for detection of genetic material.

Introduction

The natural bases of DNA are not useful as fluorescent probes because of their short absorption and emission wavelengths and extremely low quantum yields (*e.g.*, uridine exhibits λ_{abs} 260 nm, λ_{em} 308 nm, and Φ 4×10^{-5}),[1,2] and thus the use of extrinsic probes is necessary. A common methodology for the sensitive detection or quantification of RNA/DNA is the application of fluorescent dyes.[3] Currently marketed dyes[4,5] for nucleic acid staining and labeling include intercalating dyes that are incorporated non-covalently to double stranded nucleic acids,[6] minor-groove binding dyes,[7] and large hydrophobic fluorescent dyes[8] that are incorporated covalently to nucleotide (oligonucleotide) positions that do not interfere with base pairing.[8]

These dyes are used in various techniques for detecting genetic material in DNA arrays,[9] FISH,[10] gels,[11] in virus particles,[12] and in cells, by fluorescence microscopy, or in electrophoresed gels.[13]

Although the above-mentioned fluorescent dyes are useful for nucleic acid detection and quantification, they suffer from limitations regarding the preparation and application of nucleic acid probes. These limitations include: experimental procedures required prior to detection, poor solubility in water/phosphate buffer, toxicity of certain dyes,[8] and background fluorescence of unreacted dye. In addition, the large hydrophobic dye attached to a nucleotide alters the efficiency of enzymatic incorporation into DNA/RNA, resulting in different levels of labeling and prohibits quantification of nucleic acids.[9,14] A two-step protocol involving first the incorporation of a slightly modified nucleotide into nucleic acid, followed by covalent binding of fluorescent dye, also suffers from the limitation that a relatively small number of dye molecules that can be incorporated.[15,16]

The limitations and complications of current methodologies applying extrinsic dyes triggered the development of conceptually different fluorescent probes, formed by extension of the natural chromophore.[17–22]

Such intrinsically fluorescent pyrimidine nucleosides include 5-furanyl-uracil,[23,24] **1** (λ_{max} 316 nm, λ_{em} 431 nm, Φ 0.03 in H_2O), 5-pyrenyl-uracil,[25,26] **2** (λ_{max} 350 nm, λ_{em} 447 nm, Φ 0.025 in MeOH), pyrrolo 2′-deoxy-cytosine,[24,27–29] **3** (λ_{max} 353 nm, λ_{em} 448 nm, Φ 0.038 in tris buffer), phenyl pyrrolo cytosine,[30] **4** (λ_{max} 360, λ_{em} 465 nm, Φ 0.31 in phosphate buffer) (Fig. 1). These fluorescent nucleosides were incorporated into an oligonucleotide which, in turn, was used as a probe for detection of genetic material in cells. The photophysical properties of the above mentioned fluorescent nucleosides were either slightly changed or remained unchanged upon their incorporation into oligonucleotides.[23,30,31]

Department of Chemistry, Bar-Ilan University, Ramat-Gan, 52900, Israel. E-mail: bilha.fischer@biu.ac.il; Fax: 972-3-6354907; Tel: 972-3-5318303

†Electronic supplementary information (ESI) available: ^{13}C and ^{1}H NMR, as well as absorption and emission spectra of reported compounds. This material is available free of charge *via* the internet at http://pubs.acs.org. See DOI: 10.1039/c1ob06536j

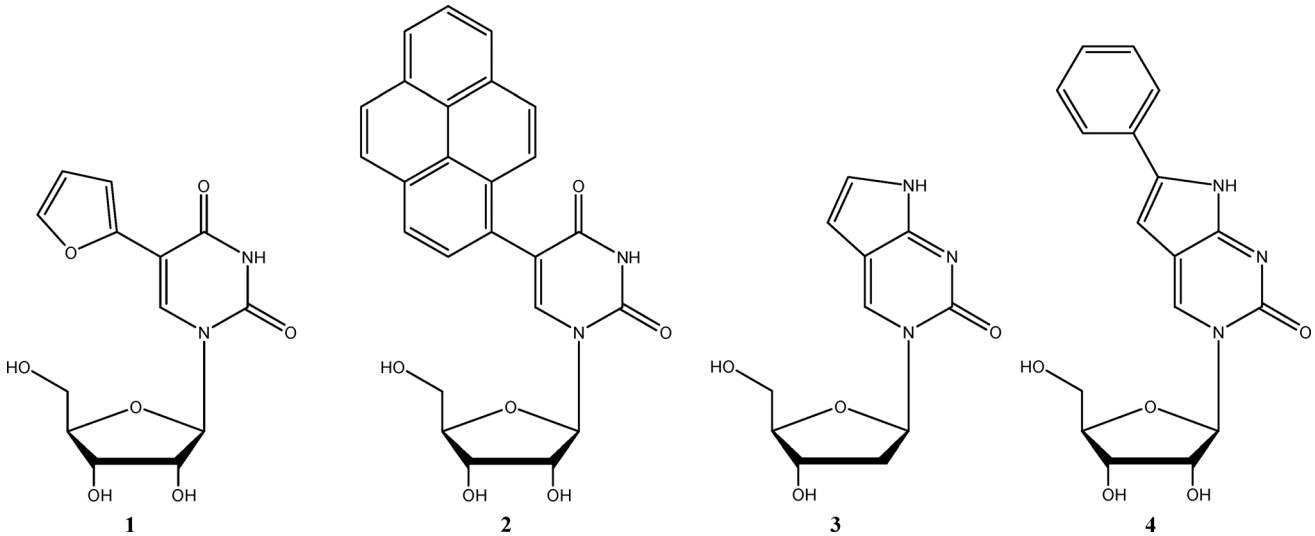

Fig. 1 Previously reported fluorescent 5-substituted pyrimidine nucleoside analogues.

The limitations of current intrinsically fluorescent uridine probes, namely, relatively short λ_{em}, low Φ values, and small differences in emission wavelengths and quantum yields between the single strand probe and the duplex, encouraged us to develop novel uridine based fluorescent probes, with improved photophysical properties.

Specifically, we targeted the development of fluorescent uridine or 2′-deoxy-uridine analogues which can replace uridine or 2′-deoxy-thymidine in RNA or DNA probes, respectively. We focused on extending the uracil chromophore by minimal chemical modification leading to a satisfactory emission wavelength and quantum yield without disturbing the H-bonding of the uracil derivative with its complementary nucleobase.

Here, we describe the design and synthesis of a novel series of push–pull uridine-based fluorescent probes, **5–8** (Fig. 2), as well as their spectroscopic and conformational properties. In addition, we analyze the structure–activity relationships of probes **5–8**, and elucidate the requirements for obtaining probes with enhanced fluorescence. Furthermore, we demonstrated the application of a 2′-deoxy-uridine analogue, **6b**, for the preparation of labeled oligonucleotide probes useful for detection of genetic material.[32]

Results

Probe design

To design fluorescent probes based on suitable extensions of the uracil chromophore, we applied the following strategies: 1) selection of minimal extensions of the natural nucleobase at positions not involved in H-bonding with a complementary base. 2) Selection of probes that may be excited and may emit at the longest possible wavelengths. 3) Selection of extensions of the uracil base that can be achieved *via* a simple and short synthesis.

Specifically, the modifications we selected included coupling uracil at the C5 position to various aromatic systems. As substituents that donate electrons to the π system enhance absorption of light and increase fluorescence,[33,34] we have coupled –OMe and –OH substituted aromatic rings to the uracil scaffold, to form analogues **5a–e**, **6a–c**, **7a–c**, and **8**. We have studied the contribution of both the type and position of the aromatic substituents on the fluorescence properties of the resulting uridine derivatives. For comparison of electronic effects on the aromatic ring, we also prepared the corresponding *p*-CF_3- substituted analogue, **6d**.

We elected to couple the aromatic substituent at the uracil C5 position, since substitution at the C6 position will drive the nucleoside into the undesired *syn* conformation.

Altogether, we prepared and characterized four types of C5 substituted uridine analogues where the aromatic systems are: a) directly coupled (**5a–e**), b) coupled *via* an alkenyl linker (**6a–c**), c) coupled *via* an alkynyl linker (**7a–c**), and d) coupled *via* a dienyl linker (**8**) (Fig. 2).

We coupled aromatic or conjugated aromatic moieties to the C5 position of uracil by the Suzuki coupling reaction to provide **5a–e**, **6a–c**, and **8**, and by the Sonogashira coupling to yield **7a–c**.

Synthesis of 5-substituted-uridine derivatives

Suzuki coupling reactions are highly useful for the preparation of biaryl compounds.[35] The Pd-catalyzed Suzuki reaction proved to be effective also for nucleoside cross-coupling,[36] and was applied here for the preparation of derivatives **5a–e**, **6a,b** and **8** from unprotected 5-iodo-uridine, 5-I-U, or 2′-deoxy-5-I-U, or 5-(2-Br-vinyl)-uridine, in one-step and in reasonably good yields (Schemes 1 and 2).[37] Thus, 5-I-U, **9a/b**, and the appropriate aryl boronic acid derivative, *e.g.*, **10a–d**, in water : acetonitrile (2 : 1) were treated with Na_2CO_3 and a catalyst system containing $Pd(OAc)_2$ and TPPTS.[37,38] Products **5a–c** were obtained in high purity after silica gel chromatography.

Similarly, compounds **6c** and **8** were prepared from 5-(2-bromovinyl)-uridine,[39,40] **13**, and 3, 4, 5-trimethoxyphenylboronic acid, **10c** and *trans*-2-(4-methoxyphenyl)-vinylboronic acid, **11a**, respectively (Scheme 2).

Products **7a–c**, where the aromatic system is linked to the uracil C5-position *via* an alkynyl moiety, were prepared by Sonogashira coupling.[41] Thus, 5-I-U, **9a**/**b**, and the appropriate alkynyl compound, **12a–c**, in DMF, were treated with $Pd(PPh_3)_4$,

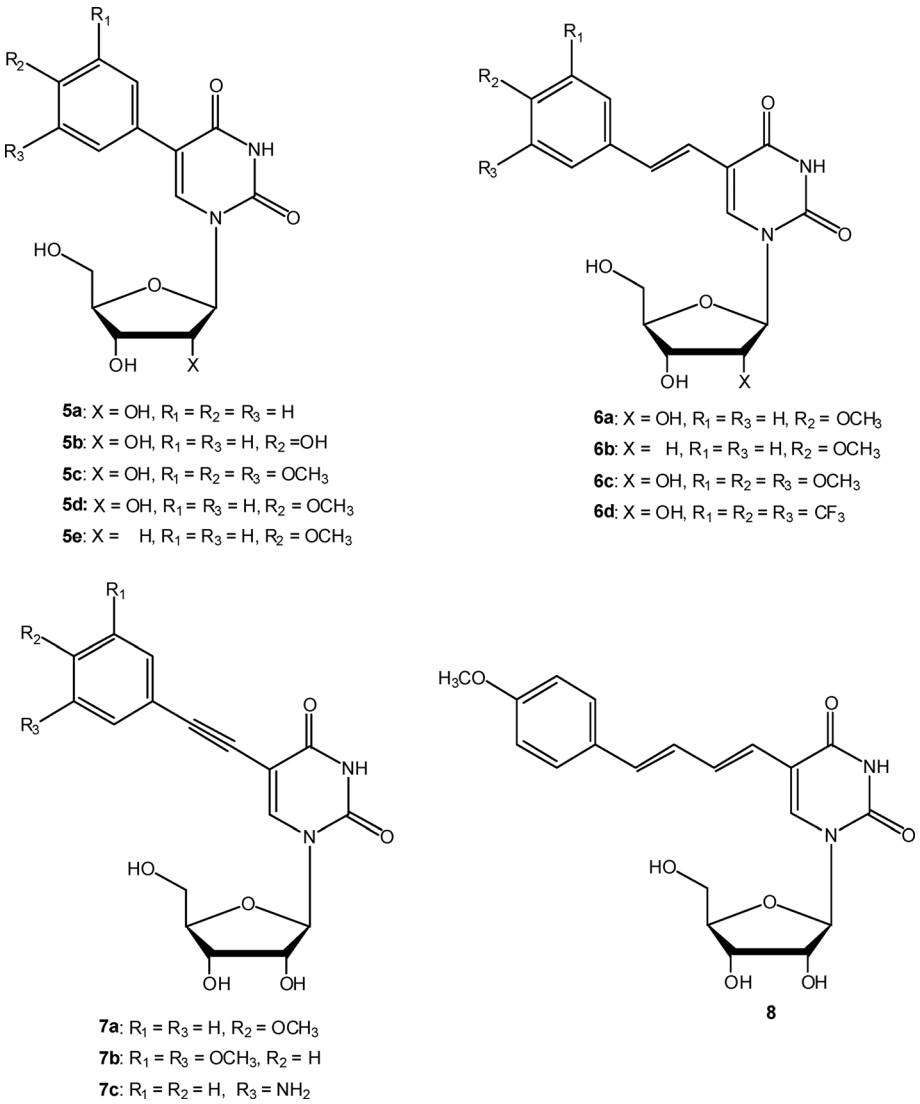

Fig. 2 Fluorescent uridine analogues synthesized and explored here.

DIPEA and CuI in the presence of TEA to obtain **7a–c** in yields between 32–74% (Scheme 3). Like the above-mentioned Suzuki reaction, the advantages of the Sonogashira reaction include the avoidance of nucleoside protection and a facile one step reaction which provides the product in a reasonable yield, upon an easy purification.

Spectral properties of uridine derivatives 5–8

We measured the absorption and emission of analogues **5–8** in MeOH or H_2O and determined their quantum yields. The selection of solvent depended on the solubility of the analogue in water. The analogues were measured preferentially in water (**6a**, **c**, **d**) if soluble, and also in MeOH, if possible (**5a**, **6b**, and **8**). The other analogues were measured in MeOH only (**5b–e**, **7a–c**).

For accurate measurements of the fluorescence, the concentrations of the samples were in the linear range in which the Beer–Lambert law applies, the optical density was less than 0.05 to avoid the inner filter effect.[42] Quantum yield (Φ_F) was calculated based on Φ of a known reference (tryptophan or quinine sulphate). λ_{abs} and λ_{em} values of the selected reference compounds were in the same range as those of the evaluated compounds.

Absorption and emission of compounds **5a–e**, **7a–c**, and **8** were measured in methanol with tryptophan[43] as a standard (Φ 0.14, λ_{abs} 280 nm, λ_{em} 350 nm). Analogues **6a–c** were measured in H_2O (pH 7) with quinine sulphate as a standard [44](Φ 0.54, λ_{abs} 350 nm, λ_{em} 446 nm) at 5 μM (OD < 0.05). The spectral data for derivatives **5–8** are summarized in Table 1. All modified nucleosides **5–8** were found to be significantly more emissive than the uridine (Table 1).

Analogues **6a–c**, in which the uracil chromophore is extended by a cinnamyl moiety, exhibited the longest absorption and emission wavelengths and highest quantum yields as compared to analogues **5a–e**, **7a–c**, and **8**. Specifically, analogue **6c** showed a 58 nm red shift of absorption wavelength as compared to uridine (λ_{abs} 260 nm) and a relatively high quantum yield–6000-times larger than that of uridine in water.[1] Furthermore, analogue **6c** showed λ_{em} of 478 nm in water, representing a 170 nm longer emission wavelength, as compared to uridine.[1]

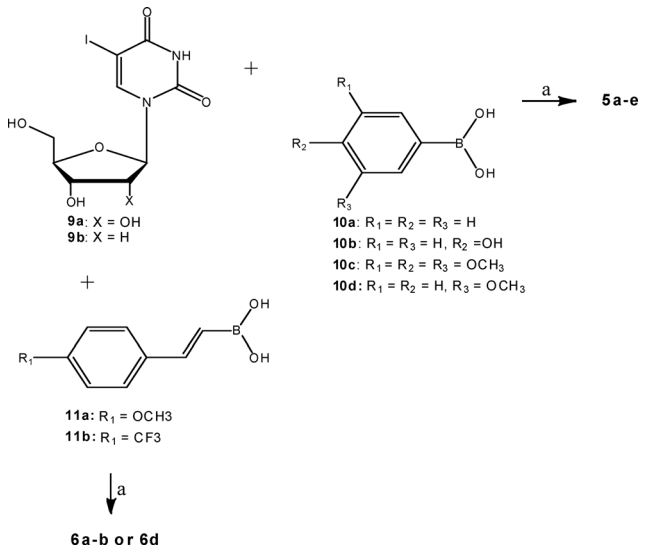

Scheme 1 Reagents and reaction conditions: a. Ar-B(OH)$_2$, 0.25 eq TPPTS, 0.05 eq Pd(OAc)$_2$, 3 eq Na_2CO_3, H_2O:CH_3CN (2 : 1), reflux, 3 h. Product yield: **5a**: 50%; **5b**: 64%; **5c**: 42%; **5d**: 13%; **5e**: 50%; **8**: 58%; **6a**: 42%; **6b**: 64% yield.

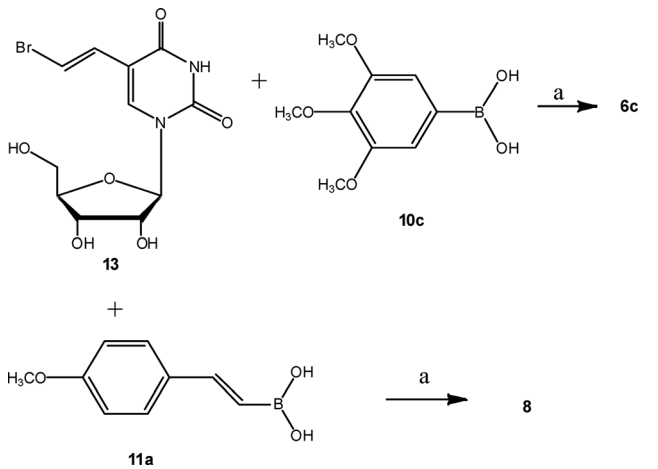

Scheme 2 Reagents and reaction conditions: a. 0.25 eq TPPTS, 0.05 eq Pd(OAc)$_2$, 3 eq Na_2CO_3, H_2O : CH_3CN (2 : 1), reflux, 3 h. **6c**: 21%; **8**: 42%.

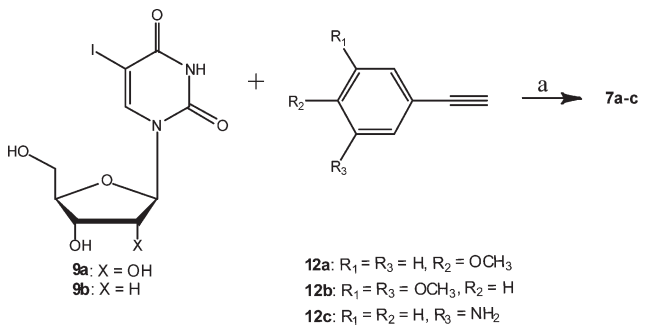

Scheme 3 Reagents and reaction conditions: a. alkyne **12a–c**, 0.2 eq CuI, 0.1 eq Pd(PPh$_3$)$_4$, 3 eq DIEAP, DMF, 18 h, RT. Product yield: **7a**: 32%; **7b**: 61%; **7c**: 74% yield.

Analogues **5a–e**, **7a–c**, and **8** showed relatively low quantum yields, ranging from 0.016–0.060. Analogues **5a–e** in which the aromatic system is directly linked to the uracil C5-position showed the least promising spectral properties with a red shift of absorption wavelength of only 25–30 nm as compared to uridine and quantum yield $\leq$ 0.06. However, the emission maximum ranged from 308 nm (for analogue **5a**), as for uridine, up to 478 nm (for analogue **5c**), representing a 170 nm shift *vs.* the emission maximum of uridine.

Table 1 Spectroscopic data for 5-substituted uridine analogues, **5–8**

Compound	λ_{abs} (nm)	λ_{em} (nm)	$\Phi^{a,b}$	Solvent
Uridine[1]	260	308	0.00004	H_2O
5a	285	308	0.020[b]	MeOH
5a	280	310	0.070[b]	H_2O
5b	290	432	0.020[b]	MeOH
5c	290	480	0.016[b]	MeOH
5d	291	420	0.030[b]	MeOH
5e	293	422	0.035[b]	MeOH
6a	328	447	0.100[a]	H_2O
6b	335	478	0.120[a]	H_2O
6b	326	477	0.036[a]	MeOH
6c	318	476	0.240[a]	H_2O
6d	288	417	0.014[b]	H_2O
7a	306	430	0.056[b]	MeOH
7b	307	408	0.032[b]	MeOH
7c	310	411	0.045[b]	MeOH
8	308	430	0.045[b]	MeOH
8	308	428	0.060[b]	H_2O

[a] Data obtained with quinine sulphate as a reference [b] Data obtained with tryptophan as a reference

Conformational analysis of uridine derivatives 5–7

A common B-DNA-like duplex is formed from nucleotides possessing the *anti* conformation only.[45] Therefore, fluorescent nucleoside analogues possessing an *anti* conformation will be favored for labeling DNA/RNA strands.

Uracil nucleosides are expected to possess conformational flexibility, due to possible rotations around the glycosidic bond and pseudorotation of the ribose ring as well as possible rotations around the C4′–C5′ bond angle (γ). However, it is well-established that most nucleosides adopt a predominant conformation in solution (which is nevertheless in equilibrium with other conformations).[46] Thus, it has been shown that a majority of purine and pyrimidine nucleosides favor an *anti* conformation of the base ring with respect to the sugar ring.[47] Likewise, the ribose ring exhibits a puckered conformation in which either the C2′ or C3′ atom is furthest from the plane of the other atoms of the ribose ring, named as south (*S*) and north (*N*) conformations, respectively.[48] Finally, it has been shown that the ribose exocyclic group exists predominantly in a *gauche–gauche* (*gg*) conformation about the C4′–C5′ bond with the O5′ atom projecting over the furanose ring.

Here, we employed ^{1}H, and ^{13}C NMR spectra to analyze the solution conformation of selected nucleoside analogues, **5d**, **6a** and **7a**.

Conformation around the glycosidic bond

Pyrimidine nucleosides can adopt two main conformations, *syn* or *anti*, in which the uracil O2 points above or away from the sugar ring. The quantitative determination of the conformation

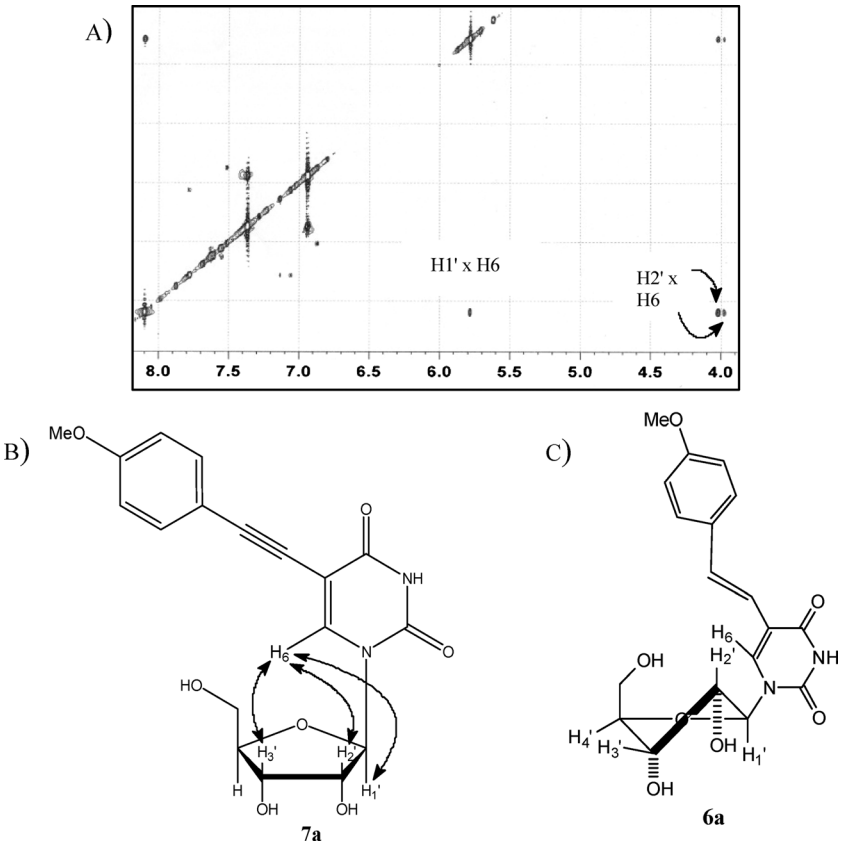

Fig. 3 A,B) NOE interactions within compound **7a**. C) Structure of compound **6a**.

around the glycosidic bond can be obtained by monitoring the vicinal coupling constants ^3JC6–H1′ and ^3JC2–H1′, which are extracted from ^{13}C NMR spectra for each nucleoside. A practical rule for the orientation of the base relative to the ribose was formulated: a value of $^3J_{C2–H1'} < {}^3J_{C6–H1'}$ indicates that χ is in the *anti* conformation, whereas the reverse indicates that χ is in the *syn* conformation.[49]

Ippel *et al.* reparametrized and generalized the Karplus equations for the glycosidic bond conformation of purine and pyrimidine nucleosides and nucleotides.[49] Eqn (1) and (2)[49] were used in this study to calculate the glycosidic bond angle χ (O4′–C1′–N1–C2) in nucleosides **5d**, **6a** and **7a** based on $^3J_{C6–H1'}$ and $^3J_{C2–H1'}$ values.[50,51]

$$^3J_{C6–H1'} = 4.5\cos^2(\chi - 60) - 0.6\cos(\chi - 60) + 0.1 \quad (1)$$

$$^3J_{C2–H1'} = 4.7\cos^2(\chi - 60) + 2.4\cos(\chi - 60) + 0.1 \quad (2)$$

These calculations give several possible χ values. In some cases we had to base our choice of χ values on additional conformational evidence. For instance, a cross peak between H-6 and H-2′/3′ in NOESY spectrum indicates an *anti* nucleotide conformation (Fig. 3).[52]

NOE interactions in compounds **5d**, **6a**, and **7b** were observed between H-6 and H-1′/2′/3′ *e.g.*, (Fig. 3A). These interactions suggest that the conformation of these compounds is *anti*, similar to the conformation of natural uridine. Moreover, all calculated χ values for the C5-substituted nucleosides **5d**, **6a** and **7b** were within the range defined as *anti* (Table 2), which concurs with previously published data.[53]

Table 2 Conformational parameters of analogues **5d**, **6a** and **7b** in DMSO-d_6 solution

Compound	Sugar puckering %*S*	Conformer population around C4′–C5′ bond			Range of χ angle
		% *gg*	% *tg*	% *gt*	
5d	54	n. d.	n. d.	n. d.	*anti*
6a	52	80	10	10	*anti*
7a	51	75	12	13	*anti*

n.d.: not determined

Sugar puckering

The conformation of the D-ribose ring of nucleosides **5d**, **6a** and **7a** was analyzed in terms of a dynamic equilibrium between two favored puckered conformations: a type *N* conformer and a type *S* conformer.[54] *N* and *S* equilibrium populations were calculated from observed $J_{1'2'}$ and $J_{3'4'}$ couplings as reported previously. According to this method, the observed vicinal couplings are related to the relative proportion of conformers by eqn (3)–(5):

$$J_{1'2'} = 9.3(1 - X_N) = 9.3X_S \quad (3)$$

$$J_{2'3'} = 4.6X_N + 5.3(1 - X_N) \quad (4)$$

$$J_{3'4'} = 9.3X_N \quad (5)$$

The mole fraction of conformers *S* and *N* can be calculated directly from the observed values of $J_{1'2'}$ and $J_{3'4'}$. Using the assigned *J*-coupling constants and the above equations, the mole fractions of conformers *S* and *N* for nucleoside **5d**, **6a** and **7a** were calculated.[51,54] Analogues **5d**, **6a** and **7d** showed a minute preference for the *S* conformer of the ribose ring (Table 2).

Conformations of the exocyclic CH_2OH group

The nucleoside coupling constants $J_{4'5'}$ and $J_{4'5''}$ can be interpreted in terms of three classical staggered rotamers, with a preferred *gauche-gauche* conformation.[53] The mole fractions of each staggered rotamer of C4′–C5′ were calculated from the following expressions (eqn (6)–(8)):

$$\rho_{gg} = [(J_t + J_g) - (J_{4'5'} + J_{4'5''})]/(J_t - J_g) \quad (6)$$

$$\rho_{tg} = (J_{4'5'} - J_g)/(J_t - J_g) \quad (7)$$

$$\rho_{gt} = (J_{4'5''} - J_g)/(J_t - J_g) \quad (8)$$

The observed proton signals, labeled H5′ and H5″, refer to downfield and upfield signals, respectively. The percentages of *gg*, *gt*, and *tg* conformers are presented in Table 2. For analogues **6a** and **7a** there is a clear preference for the *gg* rotamer around the C4′–C5′ bond, 75 and 80%, respectively (Fig. 3C). For compound **5d** the relative rotamer populations could not be determined, due to second order spectra.

Discussion

5-Substituted uridine derivatives exhibit a significant enhancement of the fluorescent properties of uridine

The presence of a rigid, planar aromatic ring system in a compound turns it to a potentially fluorescent molecule. The size of the aromatic system also affects the excitation–emission wavelength and fluorescence intensity. A few functional groups can affect the wavelength and fluorescence intensity when substituted into aromatic systems. The influence of the substitutions on the fluorescence depends not only on their location in the aromatic system but also on their tendency to donate electrons or to withdraw electrons.[55]

We targeted the preparation of push–pull uridine-containing systems to achieve a maximal enhancement of fluorescent properties triggered by a minimal chemical modification. Such molecules contain both electron rich and electron poor moieties. Since we did not know whether uracil plays the role of an electron rich or poor moiety, we synthesized analogue **6a** and **6d**, *p*-substituted by OCH_3 and CF_3, respectively. Compound **6a** proved to be a significantly more promising probe with Φ *ca.* 7-fold higher than that of **6d** and λ_{em} 30 nm longer than that of **6d** (Table 1). This observation implies that uracil plays the role of an electron poor moiety in those push–pull systems.

To understand the effect of electron donating groups (EDGs) on the quantum yield of nucleosides **5–7**, we first compared analogues **5a** and **5b**, where R_2 = H and OH, respectively. Apparently, no change in quantum yield (Φ 0.02) was due to substitution of H by an OH group. Similarly, when H was substituted by OMe as in **5d**, the quantum yield shifts only slightly from 0.02 to 0.03. *I.e.*, an EDG on the scaffold of nucleosides **5** does not increase quantum yield. Furthermore, even the substitution of three OMe groups as in **5c**, does not change the quantum yield (0.016).

Unlike nucleoside **5**, in the nucleoside **6** series, a significant additive effect of the phenyl ring substituents, in **6c** *vs.* **6a**, was observed where both Φ (0.24) and λ_{em} (476 nm) were increased for **6c**. Moreover, analogue **6c** was found to be 15-times more emissive than the related analogue **5c** (Φ 0.24 *vs.* 0.016). Apparently, it is not the aryl substituent affecting the quantum yield, but rather the fluorophore, *i.e.* 5-cinnamyl-U *vs.* 5-phenyl-U.

The effect of an EDG at the *meta* position of the aromatic ring on the fluorescence of the nucleoside analogue was studied for the alkynyl-linked analogues **7a–c**.

Compound **7a** bearing OMe at the *para* position was compared with two alkynyl analogues, **7b**, $R_1 = R_3$ = OMe and **7c**, $R_3 = NH_2$ at the *meta* positions. An EDG at the *meta* position resulted in less emissive nucleosides **7b,c** as compared to **7a** where R_2 = OMe (Φ 0.032 and 0.045 *vs.* 0.056). Namely, an EDG at the *meta* position(s) does not contribute significantly to the enhancement of the Φ value. Furthermore, nucleoside **7a** exhibits slightly improved fluorescence (Φ 0.056) *vs.* **5d** (Φ 0.030) where the aryl moiety is directly linked to uridine and also has OMe group at *para* position, probably since this analogue has a longer conjugated π-system. In the series of analogues **5d**, **6a** and **7a** which contain a *p*-OMe-phenyl group that is directly-, alkenyl-, or alkynyl- linked, respectively, the cinnamyl analogue **6a** proved to have the highest quantum yield (0.1) and longest emission wavelength (447 nm), again indicating that extending the uracil base with a cinnamyl moiety, rather than phenyl or phenalkynyl, resulted in a favored fluorophore. Surprisingly, analogue **8**, bearing a dienyl linker and a longer fluorophore, was less emissive than **6a** (see discussion below).

In conclusion, all tested uridine analogues **5–8** showed significantly improved spectral properties as compared to uridine. Analogues in which the aromatic moiety is directly coupled to uracil showed the smallest spectral changes as compared to uridine, with up to 500-fold enhancement of the quantum yield of uridine, (Φ 0.02 and λ_{em} 308 nm), while analogues where uracil was extended by a cinnamyl moiety, *e.g.*, **6c**, exhibited the most promising spectral data, up to 6000-fold enhancement of the quantum yield of uridine, (Φ 0.24 and λ_{em} 476 nm).

The enhanced fluorescence (bathochromic shift) of analogues 5–8 *vs.* uridine is due to an intramolecular charge transfer mechanism

Fluorescent uridine analogues **5–8** were designed as push–pull probes to enhance the fluorescent properties of uridine. Specifically, these analogues are composed of three moieties—an electron donor (D, an electron rich aryl group); an electron acceptor (A, uracil ring), and an electron rich linker which is a double/triple bond (as in analogues **6** and **7**), a diene (as in **8**) or a single bond (as in **5**). Analogues **5–7** belong to a group of fluorescent molecules termed 'molecular rotors', which includes 9-(dicyanovinyl) julolidine (DCVJ)[56] and *p*-(dimethylamino) stilbazolium (*p*-DASPMI).[56]

Molecular rotors respond to photoexcitation with an intramolecular charge transfer (ICT) from the donor to the acceptor unit. The electrostatic forces induce an intramolecular twisting motion of D and A units relative to each other.[42,56,57]

In addition, the charge transfer occurring in the excited state (D^+–π–A^-) results in increased dipole moment. Polar solvent molecules orient themselves along the fluorophore dipole by aligning their electric fields. Upon relaxation the solvent molecules return to the ground-state orientation resulting in a bathochromic shift of the emitted light. This shift reflects the energy expended for the reorientation of the solvent molecules, which in turn is dependent on the solvent polarity.[30,56,58] Generally, polar solvents stabilize ICT states[56] and thus increase relaxation from the ICT state. Specifically, MeOH and water form H-bonds with the molecular rotor and increase ICT formation rate.

Since uridine does not posses a typical molecular rotor structure, it does not undergo an ICT mechanism. Yet, push–pull analogues **5–8** exhibit strong ICT as reflected by a bathochromic shift of up to 170 nm (*e.g.* analogues **5c** and **6b,c**), as compared to uridine.

To enhance ICT, and hence bathochromic shift, we substituted analogue **5a** with an EDG at the *para* position (**5c**) or at the *para* and *meta* positions (**5d**). Indeed the strong ICT in **5c** resulted in 170 nm red shift as compared to uridine. A similar behavior was observed for analogues **6b** and **6c**. A strong ICT is observed with an EDG at *para* position as opposed to *meta* positions, as demonstrated by analogue **7a** (*p*-OMe; λ_{em} 430 nm) *vs.* **7b** (*m*-di-OMe; λ_{em} 408 nm). Moreover, an EWG at the *para* position (CF_3) (**6d**), resulted in a low ICT as compared to **6a–c**, substituted with an EDG. Compound **8**, bearing a dienyl linker, showed a shorter emission wavelength and a lower quantum yield as compared to **6a**. This is possibly due to the diene moiety between the acceptor unit (uracil) and the donor unit (*p*-methoxyphenyl), which enables the distribution of the negative charge in the excited state on the diene and less on the uracil acceptor, unlike in the vinyl analogue, **6a**, thus reducing ICT.

The higher quantum yields found for analogues **6a–c**, measured in water, as compared to analogues **5** and **7**, measured in MeOH, is possibly due to the higher viscosity of water (0.897 cP) *vs.* MeOH (0.544 cP). For molecular rotors the solvent viscosity is the primary determinant of fluorescent quantum yield.[42,56]

C5-Substituents have no influence on the conformation of uridine analogues

The conformation of pyrimidine nucleosides required for the formation of a B-DNA-like duplex, includes an *anti* nucleoside with *S* sugar puckering and *gg* conformer of the ribose exocyclic group.

We found that substituents at the C5 position of the uracil base did not influence the nucleoside standard conformation, probably since they exert no steric hindrance.

All χ values calculated for the C5-substituted uracil nucleosides, **5–7**, were within the range defined as *anti*, consistent with previous data that pyrimidine analogues substituted at positions other than C2 and C6 exist in a predominantly *anti* conformation.[53] Analogues **5–7** showed a slight preference for the *S* conformer of the ribose ring. Moreover, the ribose exocyclic group of these analogues exists predominantly in a *gauche–gauche* conformation about the C4′–C5′ bond (Fig. 3C).

Conclusions

In summary, based on the relatively large quantum yields, up to 6000-fold more than uridine, and long emission wavelengths of **6b**, and **6c** (Φ 0.12 and 478 nm; 0.24 and 476 nm), in addition to the uridine-like conformation of these analogues, we suggest **6b** and **6c**, as promising fluorescent probes involving an ICT mechanism. We will report shortly the incorporation of analogue **6b** into oligonucleotides and the fluorescent properties of the resulting DNA single strands and duplexes, towards the development of a new diagnostic tool.[32]

Experimental

General

Compounds were characterized by nuclear magnetic resonance using Bruker AC-200, DPX-300 or DMX-600 spectrometers. ^{1}H NMR spectra were measured at 200, 300 or 600 MHz. For conformational analysis ^{1}H-NMR and NOESY spectra were performed with DMSO-d_6 as solvent. Chemical shifts are expressed in ppm. Mass spectra were obtained on a MicroMass QTOF (Waters, UK) spectrometer (MS ESI). Progress of reactions was monitored by TLC on precoated Merck silica gel plates (60F-254). Visualization was accomplished by UV light. Medium pressure chromatography was carried out using automated flash purification system (Biotage SP1 separation system, Uppsala, Sweden). All moisture sensitive reactions were carried out in flame-dried reactions flasks with rubber septa, and the reagents were introduced with a syringe. All reactants in moisture sensitive reactions were dried overnight in a vacuum oven. Absorption spectra were measured on a UV-2401PC UV-VIS recording spectrophotometer (Shimadzu, Kyoto, Japan). Emission spectra were measured using Aminco–Bowman series 2 (AB2) Luminescence Spectrometer (Thermo electron corporation, Markham, Ontario, Canada). Samples with maximum absorbance of less than 0.05 were used to avoid inner filter distortion.

UV measurements

Absorption spectra were determined in H_2O (pH 7) for compounds **6a–c**, and MeOH for analogues **5a–c**, **7a–c**, and **8**. The concentration of the samples was 6 μM. Absorbance was kept less than 0.05 AU in order to avoid inner filter distortion. Samples were measured in a 10 mm quartz cell.

Fluorescent measurements

Emission spectra of compounds **6a–c** were determined in H_2O (pH 7) and in MeOH for compounds **5a–c**, **7a–c**, and **8**. Measurement conditions of analogues **5–8** included 740 V sensitivity and a 4 nm slit. The concentration of the samples was 6 μM. Samples were measured in a 10 mm quartz cell.

Quantum yield measurements

The quantum yield of each compound was calculated from the observed absorbance and the area of the fluorescence emission band. The fluorescence quantum yield of all nucleosides was determined relative to the quantum yield of quinine sulfate (0.58)[59] or tryptophan (0.14)[59] in H_2O (pH 7) or MeOH, respectively, according to eqn (9).

$$\Phi_F = \frac{\Phi_R I}{I_R} \times \frac{OD_R}{OD} \times \frac{\eta^2}{\eta_R} \quad (9)$$

Where R = reference, I = integration of the peak and η = refractive index of the solvent.

1-((2*R*,3*R*,4*S*,5*R*)-3,4-dihydroxy-5-(hydroxymethyl)tetrahydrofuran-2-yl)-5- phenylpyrimidine-2,4(1*H*,3H)-dione (5a) - A typical procedure

Water : acetonitrile (2 : 1, 1.6 mL) was added through a septum to a nitrogen-purged round bottom flask containing **9a** (100 mg, 0.27 mmol), phenylboronic acid (41.15 mg, 0.33 mmol), $Pd(OAc)_2$ (3 mg, 0.01 mmol), TPPTS (38.37 mg, 0.06 mmol) and Na_2CO_3 (85.85 mg, 0.81 mmol). The mixture was stirred under reflux for 3 h and monitored by TLC (8 : 2 $CHCl_3$: MeOH). The solvent was evaporated and water was added. The resulting solution was freeze dried. The residue was separated on a silica gel column (90 : 10 $CHCl_3$: MeOH). Product **5a** was obtained as a white solid in a 50% yield (43.4 mg). ^{1}H NMR (300 MHz, CD_3OD): δ 8.34 (s, 1H) 7.56–7.53 (m, 2H), 7.38–7.31 (m, 4 H), 6.50 (m, 1H), 5.99 (d, J = 4.2 Hz, 1H), 4.23–4.21 (m, 2H), 4.03 (m, 1H), 3.89–3.71 (m, 2H) ppm. ^{13}C NMR (600 MHz , DMSO d_6) δ 164.62, 141.48, 139.93, 129.54, 129.39, 129.30, 128.64, 116.08, 90.92, 86.26, 80.15, 76.08, 71.12, 63.00, 61.85. ESI+ MS *m*/*z*: 343 (MNa^+). Analysis calculated for $C_{15}H_{16}N_2O_6$: C 56.37, H 5.01, N 8.77, O 30.06. Found: C 55.97, H 4.68, N 8.57, O 29.65.

1-((2*R*,3*R*,4*S*,5*R*)-3,4-dihydroxy-5-(hydroxymethyl)tetrahydrofuran-2-yl)-5-(4-hydroxyphenyl)pyrimidine-2,4(1*H*,3H)-dione (5b)

Product **5b** was obtained from **9a** (100 mg, 0.27 mmol) and 4-hydroxyphenylboronic acid (58.38 mg, 0.33 mmol) following the above procedure. Product **5b** was obtained as a white solid in a 64% yield (58 mg). ^{1}H NMR (300 MHz, CD_3OD): δ 8.61 (s, 1H), 7.4 (d, J = 4.4, 2H), 6.8 (d, J = 4.2 Hz 2H), 6.5 (m, 1H), 5.99 (d, J = 4.75, 1H), 4.25–4.16 (m, 2H), 4.0 (m, 1H), 3.85–3.76 (m, 2H) ppm. ESI+ MS *m*/*z*: 359 (MNa^+). Analysis calculated for $C_{15}H_{16}N_2O_7$: C 53.57, H 4.80, N 8.33, O 33.30. Found: C 53.29, H 4.51, N 7.97, O 32.9.

1-((2*R*,3*R*,4*S*,5*R*)-3,4-dihydroxy-5-(hydroxymethyl)tetrahydrofuran-2-yl)-5-(3,4,5-trimethoxyphenyl)pyrimidine-2,4(1*H*,3H)-dione (5c)

Product **5c** was obtained from **9b** (100 mg, 0.27 mmol) and 3, 4, 5- trimethoxybenzeneboronic acid (74.2 mg, 0.35 mmol) following the above procedure. Product **5c** was obtained as a white solid in a 42% yield (42.7 mg). ^{1}H NMR (300 MHz , DMSO d_6): δ 8.14 (s, 1H), 6.85 (s, 2H), 6.24 (t, J = 7.43 Hz, 1H), 5.76 (d, J = 4.9,1H), 4.39 (m, 1H), 3.80 (s, 6H), 3.72 (s, 3H), 2.27 (m, 2H) ppm. ^{13}C NMR (00 MHz , DMSO d_6) δ 162.01, 152.51, 149.82, 137.92, 136.92, 113.26, 105.37, 87.67, 84.61, 70.24, 61.02, 60.02, 55.85. ESI+ MS *m*/*z*: 410 (MH^+). Analysis calculated for $C_{18}H_{22}N_2O_9$: C 52.68, H 5.36, N 6.83, O 35.12. Found: C 52.92, H 5.22, N 7.23, O 35.41

1-((2*R*,3*R*,4*S*,5*R*)-3,4-dihydroxy-5-(hydroxymethyl)tetrahydrofuran-2-yl)-5-(4-methoxyphenyl)pyrimidine-2,4(1*H*,3H)-dione (5d)

Product **5d** was obtained from **9a** (100 mg, 0.27 mmol) and 4-methoxy-phenylboronic acid (53 mg, 0.35 mmol) following the above procedure. Product **5d** was obtained as a white solid in a 13% yield (12.5 mg). ^{1}H NMR (300 MHz , DMSO d_6): δ 11.39 (br. s, 1H), 8.15 (s, 1H), 7.49 (d, J = 9 Hz, 2H) 6.93 (d, J = 8.9 Hz, 2H), 5.86 (d, J = 4.8 Hz, 1H), 5.86 (br. s, 1H), 5.34 (br. s, 1H), 5.12 (br. s, 1H), 4.14 (m, 1H), 4.04 (m, 1H), 3.89 (m, 1H), 3.76 (s, 3H), 3.66 (m, 2H) ppm. ^{13}C NMR (600 MHz , DMSO d_6) δ 162.22, 158.51, 150.17, 137.03, 129.06, 125.33, 113.55, 113.20, 88.16, 84.72, 73.88, 69.67, 60.44, 55.09. ESI+ MS *m*/*z*: 351 (MH^+). Analysis calculated for $C_{16}H_{18}N_2O_7$: C 54.86, H 5.18, N 8.00, O 31.97. Found: C 54.51, H 5.36, N 8.25, O 31.65.

1-((2*R*,4*S*,5*R*)-4-hydroxy-5-(hydroxymethyl)tetrahydrofuran-2-yl)-5-(4-methoxyphenyl)pyrimidine-2,4(1*H*,3H)-dione (5e)

Product **5e** was obtained from **9b** (100 mg, 0.27 mmol) and 4-methoxy-phenylboronic acid (53 mg, 0.35 mmol) following the above procedure. Product **5e** was obtained as a white solid in a 50% yield (47.6 mg). ^{1}H NMR (300 MHz , DMSO d_6): δ 8.16 (s, 1H), 7.47 (d, J = 9 Hz, 2H), 6.91 (d, J = 8.9 Hz, 2H), 6.33 (t, J = 6.31 Hz, 1H), 4.42 (m, 1H), 3.95 (m, 1H), 3.78 (m, 5H), 2.28 (m, 2H) ppm. ^{13}C NMR (600 MHz , DMSO d_6) δ 162.24, 158.54, 149.93, 136.93, 125.44, 113.57, 87.48, 84.41, 70.29, 61.04, 55.11. ESI+ MS *m*/*z*: 335 (MH^+). Analysis calculated for $C_{16}H_{18}N_2O_6$: C 57.48, H 5.43, N 8.38, O 28.71. Found: C 56.98, H 5.12, N 9.02, O 28.35.

1-((2*R*,3*R*,4*S*,5*R*)-3,4-dihydroxy-5-(hydroxymethyl)tetrahydrofuran-2-yl)-5-(4-methoxystyryl)pyrimidine-2,4(1*H*,3H)-dione (6a)

Product **6a** was obtained from **9a** (100 mg, 0.27 mmol) and 2-((4-methoxy-phenyl)-*trans*-vinyl-boronic acid (62.75 mg, 0.35 mmol) following the above procedure. Product **6a** was obtained as a white solid in a 42% yield (42.7 mg). ^{1}H NMR (300 MHz, CD_3OD): δ 8.32 (s, 1H), 7.4 (d, J = 8.7 Hz, 2H), 7.3 (d, J = 16 Hz, 1 H), 6.87 (d, J = 8.7 Hz, 2H), 6.71 (d, J = 16 Hz, 1H), 5.94 (d, J = 3.94, 1H), 4.23–4.22 (m, 2H), 4.06–4.04 (m, 1H), 3.93–3.76 (m, 2H), 3.82 (s, 3H) ppm. ^{13}C NMR (600 MHz , DMSO d_6) δ 162.21, 158.76, 149.74, 137.07, 130.03, 127.32, 127.27, 118.247, 111.05, 88.18, 84.58, 73.82, 69.39, 60.41, 55.13. ESI+ MS *m*/*z*: 377 (MH^+). Analysis calculated for

$C_{18}H_{20}N_2O_7$: C 57.44, H 5.36, N 7.44, O 29.76. Found: C 57.24, H 5.20, N 7.60, O 29.35.

1-((2*R*,4*S*,5*R*)-4-hydroxy-5-(hydroxymethyl)tetrahydrofuran-2-yl)-5-(4-methoxystyryl)pyrimidine-2,4(1*H*,3H)-dione (6b)

Product **6b** was obtained from **9b** (100 mg, 0.27 mmol) and 2-((4-methoxy-phenyl)-*trans*-vinyl-boronic acid (62.74 mg, 0.35 mmol) following the above procedure. Product **6b** was obtained as a white solid in a 64%yield (65.6 mg).^{1}H NMR (300 MHz, DMSO d_6): δ 11.47 (bs, 1H), 8.17 (s, 1H), 7.41 (d, J = 2 Hz, 2 H), 7.35 (d, J = 16.8 Hz, 1H), 6.93 (d, J = 2 Hz, 2H), 6.76 (d, J = 16.8 Hz, 1H), 6.19 (t, J = 3.5 Hz, 1H), 5.28 (d, 1H), 5.19 (t, 1H), 4.29 (m, 1H), 4.11 (m, 1H), 3.76 (s, 3H), 3.7–3.6 (m, 2H), 2.17 (m, 2H) ppm. ^{13}C NMR (600 MHz , DMSO d_6) δ 162.70, 159.11, 149.93, 137.12, 130.46, 127.58, 127.46, 118.91, 117.70, 87.68, 84.73, 70.13, 61.14, 55.07, 40.42. ESI+ MS m/z: 361 (MH^+). Analysis calculated for $C_{18}H_{20}N_2O_6$: C 59.83, H 5.54, N 7.75, O 26.59. Found: C 59.43, H 5.19, N 7.5, O 26.43.

1-((2*R*,3*R*,4*S*,5*R*)-3,4-dihydroxy-5-(hydroxymethyl)tetrahydrofuran-2-yl)-5-(3,4,5-trimethoxystyryl)pyrimidine-2,4(1*H*,3H)-dione (6c)

Product **6c** was obtained from **13** (100 mg, 0.28 mmol) and 2-((4-methoxy-phenyl)-*trans*-vinyl-boronic acid (62.7 mg, 0.35 mmol) following the above procedure. Product **6c** was obtained as a white solid in a 21% yield (27 mg). ^{1}H NMR (300 MHz, DMSO d_6): δ 8.18 (s, 1H), 7.29 (d, J = 16.74 Hz, 1H), 6.74 (d, J = 16.8 Hz, 1H), 6.74 (s, 2H), 5.83 (d, 3.3 Hz, 1H), 4.17 (m, 2H), 4.05 (m, 1H), 3.98 (m, 8H), ppm. ESI+ MS m/z: 459 (MNa^+).

1-((2*R*,3*R*,4*S*,5*R*)-3,4-dihydroxy-5-(hydroxymethyl)tetrahydrofuran-2-yl)-5-((*E*)-4-(trifluoromethyl)styryl)pyrimidine-2,4(1*H*,3H)-dione (6d)

Product **6d** was obtained from **9b** (100 mg, 0.27 mmol) and 2-((4-trifluoromethyl-phenyl)-*trans*-vinylboronic acid (75 mg, 0.35 mmol) following the above procedure. Product **6b** was obtained as a white solid in a 27% yield (30 mg). ^{1}H NMR (300 MHz, DMSO d_6): δ 11.56 (br. s, 1H), 8.28 (s, 1H), 7.68 (s, 4H), 7.52 (J = 16.2 Hz, 1H), 7.08 (d, J = 14.7 Hz, 1H), 6.20 (t, J = 6.3 Hz, 1H), 5.28 (d, J = 3.6 Hz, 1H), 5.20 (t, 1H, J = 3.6 Hz), 4.29 (m, 1H), 4.10 (m, 1H), 3.82 (m, 2H), 3.32 (s, 3H), 2.18 (m, 2H) ppm. NMR (600 MHz , DMSO d_6) δ 162.04, 149.40, 141.68, 139.36, 129.11, 126.82, 126.45, 125.82, 125.53, 124.36, 110.24, 87.50, 84.53, 69.92, 60.96. ESI+ MS m/z: 397 (MH^+).

1-((2*R*,3*R*,4*S*,5*R*)-3,4-dihydroxy-5-(hydroxymethyl)tetrahydrofuran-2-yl)-5 ((1*E*,3*E*)-4-(4-methoxyphenyl)buta-1,3-dien-1-yl) pyrimidine-2,4(1*H*,3H)-dione (8)

Product **8** was obtained from **13** (63 mg, 0.18 mmol) and 2-((4-methoxy-phenyl)-*trans*-vinyl-boronic acid (40 mg, 0.25 mmol) following the above procedure. Product **8** was obtained as a white solid in a 48% yield (35 mg). ^{1}H NMR (300 MHz, DMSO d_6): δ 8.14 (s, 1H), 7.41 (m, 2H), 7.39 (d, J = 16.7 Hz, 1H), 6.86 (m, 2H), 6.61 (d, J = 15.3 Hz, 1H), 6.33 (d, J = 15.3 Hz, 1H), 6.65 (d, J = 16.8 Hz, 1H), 6.74 (s, 2H), 5.86 (d, J = 3.0 Hz, 1H), 4.22 (m, 2H), 4.01 (m, 1H), 3.83–3.72 (m, 5H) ppm. ESI+ MS m/z: 425 (MNa^+).

1-((2*R*,3*R*,4*S*,5*R*)-3,4-dihydroxy-5-(hydroxymethyl)tetrahydrofuran-2-yl)-5-((4-methoxyphenyl)ethynyl)pyrimidine-2,4(1*H*,3H)-dione (7a) - A typical procedure

Tetrakis(triphenylphosphine)palladium(0) (62 mg, 0.05 mmol), copper(I) iodide (2.6 mg, 0.11 mmol), diisopropylethylamine (0.2 mL) and 4-ethynyl anisole (0.21 mL, 1.62 mmol) were added to a solution of **9a** (200 mg, 0.54 mmol) in anhydrous DMF (16 mL). The reaction mixture was stirred at room temperature overnight under nitrogen atmosphere. After 18 h no starting material was detected by TLC (8 : 2 CH_2Cl_2 : MeOH). The solvent was evaporated and the residue was purified on a silica gel column using CH_2Cl_2 : MeOH (80 : 20) yielding **7a** as a pale yellow solid in a 32% yield (66 mg). ^{1}H NMR (300 MHz, DMSO-d_6): δ 11.723 (br. s, 1H) 8.40 (s, 1H), 7.42 (d, J = 8.4 Hz, 2 H), 6.97 (d, J = 8.7 Hz, 2H), 5.78 (d, J = 4.8 Hz, 1H), 5.44 (d, J = 5.1 Hz, 1H), 5.25 (t, J = 4.4 Hz, 1H), 5.08 (d, J = 5.4 Hz, 1H), 4.08 (m, 1H), 4.06 (m, 1H), 3.87 (m, 1H), 3.78 (s, 3H), 3.68–3.60 (m, 2H) ppm. ^{13}C NMR (600 MHz , DMSO d_6) δ 167.22, 158.98, 153.92 142.7480, 132.60, 132.53, 115.35, 114.28, 98.45, 90.39, 88.66, 84.31, 73.82, 69.55, 60.64, 55.24. ESI+ MS m/z: 375 (MH^+). Analysis calculated for $C_{18}H_{18}N_2O_7$: C 57.75, H 4.85, N 7.48, O29.92. Found: C 57.42, H 5.03, N 7.12, O 29.52.

1-((2*R*,3*R*,4*S*,5*R*)-3,4-dihydroxy-5-(hydroxymethyl)tetrahydrofuran-2-yl)-5-((3,5-dimethoxyphenyl)ethynyl)pyrimidine-2,4(1*H*,3H)-dione (7b)

Product **7b** was obtained from **9a** (200 mg, 0.54 mmol) and 1-ethynyl-3,5-dimethoxybenzene (262.7 mg, 1.62 mmol) following the above procedure. Product **7b** was obtained as a brown solid in a 61% yield (133 mg).^{1}H NMR (300 MHz, DMSO-d_6): δ 11.723 (br. s, 1H), 8.48 (s, 1H), 6.6 (m, 1 H), 6.5 (m, 1H), 5.76 (d, J = 4.2 Hz, 1H), 5.46 (d, J = 5.1 Hz, 1H), 5.29 (t, J = 6.75 Hz, 1H), 5.10 (d, J = 5.4 Hz, 1H), 4.07 (m, 2H), 3.88 (m, 1H), 3.75 (s, 6H), 3.6 (m, 2H) ppm. ^{13}C NMR (600 MHz , DMSO d_6) δ 161.35, 160.40, 149.65, 144.24, 123.83, 108.87, 101.65, 98.04, 88.50, 84.69, 82.04, 73.95, 69.21, 60.14, 55.93. ESI+ MS m/z: 405 (MH^+). Analysis calculated for $C_{19}H_{20}N_2O_8$: C 56.43, H 4.99, N 6.93, O 31.65. Found: C 56.03, H 4.80, N 7.03, O 31.33.

5-((3-aminophenyl)ethynyl)-1-((2*R*,3*R*,4*S*,5*R*)-3,4-dihydroxy-5-(hydroxymethyl)tetrahydrofuran-2-yl)pyrimidine-2,4(1*H*,3H)-dione (7c)

Product **7b** was obtained from **9a** (200 mg, 0.54 mmol) and 3-ethynylaniline (0.17 ml, 1.62 mmol) following the above procedure. Product **7b** was obtained as a brown solid in a 74% yield (144 mg). ^{1}H NMR (300 MHz, DMSO-d_6): δ 11.68 (br. s, 1H), 8.39 (s, 1H), 7.01 (t, J = 3.2 Hz, 1 H), 6.5 (m, 1H), 6.65 (m, 1 H),

6.59 (m, 1H) 5.7 (d, J = 4.8 Hz, 1H), 5.45 (d, J = 6 Hz, 1H), 5.25 (m, 1H), 5.09 (d, J = 5.4 Hz, 1H), 4.11–4.07 (m, 2H), 4.04–43.99 (m, 1H), 3.87–3.86 (s, 1H), 3.69–3.56 (m, 2H) ppm. ^{13}C NMR (600 MHz , DMSO d_6) δ 161.48, 149.73, 148.78, 143.58, 129.18, 122.60, 118.69, 116.07, 114.52, 98.59, 92.89, 88.40, 84.81, 80.86, 73.93, 69.39, 60.31. ESI+ MS m/z: 360 (MH^+). Analysis calculated for $C_{17}H_{17}N_3O_6$: C 56.82, H 4.77, N 11.69, O 26.72. Found: C 56.46, H 4.55, N 11.21, O 26.32.

References

1 S. Udenfriend and P. Zaltzman, *Anal. Biochem.*, 1962, **3**, 49–59.
2 P. R. Callis, *J. Chem. Soc., Chem. Commun.*, 1983, **34**, 329–357.
3 X. Fei and Y. Gu, *Prog. Nat. Sci.*, 2009, **19**, 1–7.
4 R. P. Haugland, *Handbook of fluorescent probes and research products; Molecular probes*, 2002.
5 R. F. Delgadillo and L. J. Parkhurst, *Photochem. Photobiol.*, **86**, 261–272.
6 L. J. L. Shi, Mao Min, Li Gang, Li Cheng Yao and Zhang Jin Gang, *Chinese Journal of Agricultural Biotechnology*, 2009, **6**, 55–59.
7 M. Munde, M. Ismail, R. Arafa, P. Peixoto, C. J. Colla, Y. L. Liu, A. Lansiaux, C. Bailly, D. W. Boykin and W. D. Wilson, *J. Am. Chem. Soc.*, 2007, **129**, 13732–13743.
8 R. T. Ranasinghe and T. Brown, *Chem. Commun.*, 2005, 5487–5502.
9 R. Pribylova, P. Kralik and I. Pavlik, *Mol. Biotechnol.*, 2009, **42**, 30–40.
10 A. Arvey, A. Hermann, C. C. Hsia, E. Ie, Y. Freund and W. McGinnis, *Nucleic Acids Res.*, 2010, **38**, e115-111–e115-117.
11 M. B. Wabuyele and S. A. Soper, *Single Mol.*, 2001, **2**, 13–21.
12 C. Beer and M. Wirth, *Anim. Cell Technol.*, 2005, 321–324.
13 R. Venkat and S. Knisley, *J. Biomed. Opt.*, 2006, **11**, 024019.
14 J. Ibach and S. Brakmann, *Angew. Chem., Int. Ed.*, 2009, **48**, 4683–4685.
15 W. Lv, X. D. Chen, D. Aumiler and A. D. Xia, *Sci. China, Ser. B: Chem.*, 2009, **52**, 1148–1153.
16 M. E. Sanborn, B. K. Connolly, K. Gurunathan and M. Levitus, *J. Phys. Chem. B*, 2007, **111**, 11064–11074.
17 D. W. Dodd and R. H. E. Hudson, *J. Org. Chem.*, 2009, **6**, 378–391.
18 R. H. E. Hudson and A. Ghorbani-Choghamarani, *Org. Biomol. Chem.*, 2007, **5**, 1845–1848.
19 R. H. E. Hudson and J. M. Moszynski, *Synlett*, 2006, 2997–3000.
20 R. H. E. Hudson and A. K. Dambenieks, *Heterocycles*, 2006, **68**, 1325–1328.
21 L. M. Wilhelmsson, A. Holmen, P. Lincoln, P. E. Nielsen and B. Norden, *J. Am. Chem. Soc.*, 2001, **123**, 2434–2435.
22 R. Sirivolu Venkata, P. Chittepu and F. Seela, *Chem. biochem.*, 2008, **9**, 2305–2316.
23 N. J. Greco and Y. Tor, *Tetrahedron*, 2007, **63**, 3515–3527.
24 R. H. E. Hudson, A. K. Dambenieks and J. M. Moszynski, *Proc. SPIE–Int. Soc. Opt. Eng.*, 2005, **5969**, 59690J-59691–59690J-59610.
25 T. L. Netzel, M. Zhao, K. Nafisi, J. Headrick, M. S. Sigman and B. E. Eaton, *J. Am. Chem. Soc.*, 1995, **117**, 9119–9128.
26 A. Cuppoletti, Y. Cho, J. S. Park, C. Strassler and E. T. Kool, *Assay Drug Dev. Technol.*, 2005, **3**, 449–450.
27 R. H. E. Hudson, A. K. Dambenieks and R. D. Viirre, *Nucleosides, Nucleotides Nucleic Acids*, 2005, **24**, 581–584.
28 D. A. Berry, K. Y. Jung, D. S. Wise, A. D. Sercel, W. H. Pearson, H. Mackie, J. B. Randolph and R. L. Somers, *Tetrahedron Lett.*, 2004, **45**, 2457–2461.
29 C. Liu and C. T. Martin, *J. Biol. Chem.*, 2002, **277**, 2725–2731.
30 A. S. Wahba, A. Esmaeili, M. J. Damha and R. Hudson, *Nucleic Acids Res.*, 2010, **38**, 1048–1056.
31 C. Wanninger-Weiss and H. A. Wagenknecht, *Eur. J. Org. Chem.*, 2008, 64–71.
32 M. Segal, E. Yavin, P. Kafri, Y. Shav-Tal, and B. Fischer, unpublished results
33 L. A. Strait, R. Ketcham, D. Jambotkar and V. P. Shah, *J. Am. Chem. Soc.*, 1964, **86**, 4628–4630.
34 G. Liu, S. Pu and X. Wang, *Tetrahedron Lett.*, 2010, **66**, 8862–8871.
35 L. Yin and J. Liebscher, *Chem. Rev.*, 2007, **107**, 133–173.
36 A. G. Firth, I. J. Fairlamb, K. Darley and C. G. Baumann, *Tetrahedron Lett.*, 2006, **47**, 3529–3533.
37 A. Collier and G. K. Wagner, *Synth. Commun.*, 2006, **36**, 3713–3721.
38 P. Capek, R. Pohl and M. Hocek, *Org. Biomol. Chem.*, 2006, **4**, 2278–2284.
39 E. De Clercq, C. Desgranges, P. Herdewijn, I. S. Sim, A. S. Jones, M. J. McLean and R. T. Walker, *J. Med. Chem.*, 1986, **29**, 213–217.
40 R. Kumar, L. Xu, E. E. Knaus, L. I. Wiebe, D. R. Tovell, D. L. Tyrrell and T. M. Allen, *J. Med. Chem.*, 1990, **33**, 717–723.
41 J. H. Cho, C. D. Prickett and K. H. Shaughnessy, *J. Org. Chem.*, 2010, 3678–3683.
42 J. R. Lakowicz, *Principles of fluorescent spectroscopy*, Baltimore, Maryland, Second Edition edn, 1986.
43 E. P. Kirby and R. F. Steiner, *J. Phys. Chem.*, 1970, **74**, 4480–4490.
44 W. H. Melhuish, *J. Phys. Chem.*, 1961, **65**, 229–235.
45 K. Umemoto, M. H. Sarma, G. Gupta and R. H. Sarma, *Biochemistry*, 1990, **29**, 4714–4722.
46 W. Saenger, in *Principles of Nucleic Acid Structure*, Springer-Verlag, New York, 1984, pp. 107–110.
47 J. T. Donohue and N. Kenneth, *Chem. Rev.*, 1960, **2**, 363–371.
48 M. Sundaralingam, *Biopolymers*, 1969, **7**, 821–860.
49 J. H. Ippel, S. S. Wijmenga, R. Jong, H. A. Heus, C. W. Hilbers, E. Vroom, G. A. Marel and J. H. Van Boom, *Magn. Reson. Chem.*, 1996, **34**, S156–S176.
50 C. Altona and M. Sundaralingam, *J. Am. Chem. Soc.*, 1972, **94**, 8205–8212.
51 D. B. Davies and S. S. Danyluk, *Biochemistry*, 1974, **13**, 4417–4434.
52 F. R. Prado, P. C. Giessner and B. Pullman, *J. Theor. Biol.*, 1978, **74**, 259–277.
53 W. Uhl, J. Reiner and H. G. Gassen, *Nucleic Acids Res.*, 1983, **11**, 1167–1180.
54 C. Altona and M. Sundaralingam, *J. Am. Chem. Soc.*, 1973, **95**, 2333–2344.
55 M. Furst, H. Kallmann and F. H. Brown, *J. Chem. Phys.*, 1957, **26**, 1321–1332.
56 M. A. Haidekker and E. A. Theodorakis, *J. Biol. Eng.*, 2010, **4**, 1754–1611.
57 H.-A. Wagenknecht, *Nat. Prod. Rep.*, 2006, **23**, 973–1006.
58 R. Nandy and S. Sankararaman, *Beilstein J. Org. Chem.*, 2010, **6**, 992–1001 No 1112
59 *A Guide to recording fluorescence quantum yields*, Jobin Yvon Ltd., Dalston Gardens, Stanmore, UK.